



日本原子力研究開発機構機関リポジトリ
Japan Atomic Energy Agency Institutional Repository

Title	Numerical study of plasma generation process and internal antenna heat loadings in J-PARC RF negative ion source
Author(s)	Shibata Takanori, Nishida Kenjiro, Mochizuki Shintaro, Mattei S., Lettry J., Hatayama Akiyoshi, Ueno Akira, Oguri Hidetomo, Okoshi Kiyonori, Ikegami Kiyoshi, Takagi Akira, Asano Hiroyuki, Naito Fujio
Citation	Review of Scientific Instruments, 87(2), p.02B128_1-02B128_3
Text Version	Publisher's Version
URL	https://jopss.jaea.go.jp/search/servlet/search?5053103
DOI	https://doi.org/10.1063/1.4931787
Right	<p>This article may be downloaded for personal use only. Any other use requires prior permission of the author and the American Institute of Physics.</p> <p>The following article appeared in Review of Scientific Instruments and may be found at https://doi.org/10.1063/1.4931787.</p>

Numerical study of plasma generation process and internal antenna heat loadings in J-PARC RF negative ion source

T. Shibata, K. Nishida, S. Mochizuki, S. Mattei, J. Lettry, A. Hatayama, A. Ueno, H. Oguri, K. Ohkoshi, K. Ikegami, A. Takagi, H. Asano, and F. Naito

Citation: [Review of Scientific Instruments](#) **87**, 02B128 (2016); doi: 10.1063/1.4931787

View online: <http://dx.doi.org/10.1063/1.4931787>

View Table of Contents: <http://scitation.aip.org/content/aip/journal/rsi/87/2?ver=pdfcov>

Published by the [AIP Publishing](#)

Articles you may be interested in

[Analysis of rapid increase in the plasma density during the ramp-up phase in a radio frequency negative ion source by large-scale particle simulationa\)](#)

Rev. Sci. Instrum. **85**, 02B126 (2014); 10.1063/1.4858136

[Numerical study of the inductive plasma coupling to ramp up the plasma density for the Linac4 H⁻ ion sourcea\)](#)

Rev. Sci. Instrum. **85**, 02B113 (2014); 10.1063/1.4833920

[Spallation neutron source saddle antenna H⁻ ion source projecta\)](#)

Rev. Sci. Instrum. **81**, 02A709 (2010); 10.1063/1.3277183

[Global equilibrium in electron cyclotron resonance ion sources](#)

Rev. Sci. Instrum. **77**, 03A340 (2006); 10.1063/1.2169701

[Characteristics of multiantenna rf ion source](#)

Rev. Sci. Instrum. **75**, 1841 (2004); 10.1063/1.1702138



JANIS

**Janis Dilution Refrigerators & Helium-3 Cryostats
for Sub-Kelvin SPM**

Click here for more info www.janis.com/UHV-ULT-SPM.aspx

Numerical study of plasma generation process and internal antenna heat loadings in J-PARC RF negative ion source

T. Shibata,^{1,a)} K. Nishida,² S. Mochizuki,² S. Mattei,³ J. Lettry,³ A. Hatayama,² A. Ueno,¹ H. Oguri,¹ K. Ohkoshi,¹ K. Ikegami,¹ A. Takagi,¹ H. Asano,¹ and F. Naito¹

¹*J-PARC Center, Tokai-mura, Naka-gun, Ibaraki-ken 319-1195, Japan*

²*Keio University, Hiyoshi, Kohoku-ku, Yokohama-shi, Kanagawa-ken 223-8522, Japan*

³*European Organization for Nuclear Research (CERN), 1211 Geneva 23, Switzerland*

(Presented 25 August 2015; received 22 August 2015; accepted 4 September 2015; published online 4 November 2015)

A numerical model of plasma transport and electromagnetic field in the J-PARC (Japan Proton Accelerator Research Complex) radio frequency ion source has been developed to understand the relation between antenna coil heat loadings and plasma production/transport processes. From the calculation, the local plasma density increase is observed in the region close to the antenna coil. Electrons are magnetized by the magnetic field line with absolute magnetic flux density 30–120 Gauss which leads to high local ionization rate. The results suggest that modification of magnetic configuration can be made to reduce plasma heat flux onto the antenna. © 2015 AIP Publishing LLC. [<http://dx.doi.org/10.1063/1.4931787>]

I. INTRODUCTION

Operation of radio frequency (RF) cesium (Cs) seeded negative ion source (IS) in J-PARC (Japan Proton Accelerator Research Complex) linear accelerator has been started from September 29, 2014. Negative hydrogen ion (H^-) beam with current up to 33 mA is extracted from the IS for 1100 hr without serious trouble. The H-current is planned to be increased to 50 mA, with a flat-top duty factor of 1.25% ($0.5 \text{ ms} \times 25 \text{ Hz}$), normalized emittance to be smaller than $1.5 \pi \text{ mm mrad}$ and a life-time of IS to be longer than 1 month.¹

In order to achieve the desired performance of H-beam, understandings and prediction of plasma production and transport mechanisms inside the IS are necessary. Numerical simulation can be a powerful tool to advance R&D without long experimental duration and large cost. In the present paper, a development of the numerical model for RF IS plasma is reported. Also, the initial calculation focused on the heat loadings of RF antenna due to plasma transport is discussed.

One of the most serious limits of H^- beam performance is the life-time of RF antenna coil. From the massive amount of experiments in Spallation Neutron Source (SNS) and in J-PARC, it has been clarified that the main causes of the antenna failure are defects or inclusions on enamel surface which take place in manufacture process.² However, the relation between transports of plasma particles and antenna failure criteria (via defects) is still not completely understood. In the present model, transport of electrons (e^-), protons (H^+), and H_2^+ is solved including the effects of inductive and capacitive electromagnetic (EM) fields, elastic and inelastic collisions between background particles (H_2 , H, Cs, H_3^+) and Coulomb collision to clarify the heat flux toward antenna coil.

II. J-PARC RF ION SOURCE

A schematic drawing of the J-PARC RF IS is shown in Fig. 1. A three turn internal antenna coil is located inside the cylindrical oxygen-free copper (OFC) chamber. The antenna coil is coated by enamel of 0.5–0.7 mm thickness. The chamber is surrounded by 18 and 4 cusp magnets installed on the side wall and on the back plate, respectively. A pair of rod-filter magnets is installed between the RF antenna coil and plasma electrode (PE) as shown in Figs. 1 and 2. Two pairs of electron suppression magnets are installed in extraction electrode. The absolute magnetic flux density by the cusp, the filter, and the electron suppression magnets are shown in Fig. 3.

Alternate current with amplitude 280 A flows in the coil circuit and alternate voltage with amplitude of 1800 V is applied between the ends of the antenna coil. The voltage amplitude is calculated from the equivalent circuit model (Fig. 3(a) in Ref. 3; coil inductance $L_{ap2} = 0.5428 \mu\text{H}$ and resistance $R_{ap2} = 1.085 \Omega$) by substituting the alternate current. The RF is $\omega_{RF} = 2.0 \text{ MHz}$.

III. NUMERICAL MODEL

The discharging conditions in the numerical model is briefly shown in Table I. H_2 gas pressure is given as 3.0 Pa with assumptions of gas temperature to be 1000 K during the discharge and dissociation degree to be 0.1. Geometry of the numerical model is two-dimensional (2D) RZ plane perpendicular to the rod-filter bar magnet in order to reproduce the effect of B field produced by the filter magnets.

In the model, equations of motions for charged particles are solved by leap-frog method,⁴

$$m_j dv_j/dt = q(\mathbf{E} + \mathbf{v}_j \times \mathbf{B}) + \mathbf{F}_{\text{coll}}, \quad (1)$$

where the subscript “j” is e^- , H^+ , and H_2^+ , respectively. The sample particles are initially given uniformly with the density in Table II. The basic calculation conditions are

Note: Contributed paper, published as part of the Proceedings of the 16th International Conference on Ion Sources, New York, New York, USA, August 2015.

^{a)}Electronic mail: shibat@post.j-parc.jp.

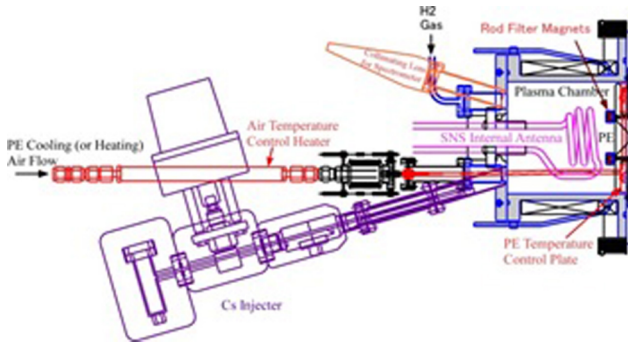
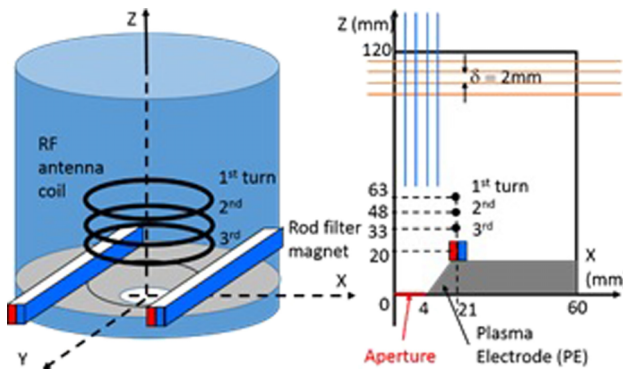
FIG. 1. Schematic drawing of J-PARC RF IS.¹

FIG. 2. Geometry of two-dimensional (2D) numerical model.

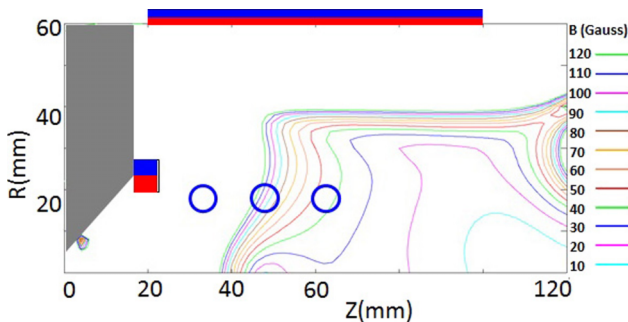


FIG. 3. Contour of absolute magnetic flux density by cusp and filter magnets.

TABLE I. Discharging conditions in the numerical model.

H ₂ gas pressure	3.0 Pa
Gas temperature (H ₂ , H, Cs)	1000 K
Dissociation degree	0.1

TABLE II. Initial particle density and calculation conditions.

Electron density	$1.0 \times 10^{15} \text{ m}^{-3}$
Proton density	$9.0 \times 10^{14} \text{ m}^{-3}$
H ₂ ⁺ density	$1.0 \times 10^{14} \text{ m}^{-3}$
Cs ⁺ density	$1.0 \times 10^{12} \text{ m}^{-3}$
Particle weight	$w = 10^6 - 10^7$
Time step width for orbit calculation	$dt = 1 \times 10^{-13} \text{ s}$
Time step width for collision calculation	$dt_{\text{coll}} = 1 \times 10^{-11} \text{ s}$
FDTD cell width	$\delta = 2 \times 10^{-3} \text{ m}$

TABLE III. Main elastic and inelastic reactions (only related to particle production and extinction).

Reaction
$e + \text{H}_2 \rightarrow 2e + \text{H}_2^+$ (H ₂ ionization)
$e + \text{H} \rightarrow 2e + \text{H}^+$ (H ionization)
$e + \text{H}_2^+ \rightarrow 2e + 2\text{H}^+$ (H ₂ ⁺ dissociative ionization)
$e + \text{H}_2^+ \rightarrow e + \text{H} + \text{H}^+$ (H ₂ ⁺ dissociation)
$e + \text{H}_2^+ \rightarrow e + 2\text{H}$ (recombination)
$e + \text{H}_2 \rightarrow 2e + \text{H} + \text{H}^+$ (H ₂ dissociative ionization)

also shown in the table. Particle orbits in the EM field are calculated each 1×10^{-13} s. Collision forces F_{coll} due to elastic/inelastic collisions between background particles and Coulomb collisions among charged particles are calculated each 1×10^{-11} s. The main elastic and inelastic collisions⁵ are listed in Table III. The stochastic processes, velocity transfer, and energy loss are calculated by applying null-collision method.⁶ The Coulomb collisions are solved by binary collision model.⁷ The Coulomb collision frequency is calculated from local charged particle density.

The 2D calculation domain is divided into small cells with 2 mm cell width. At each cell, local plasma current and density are obtained from the transport calculation. Inductive EM field produced from the antenna and the plasma currents is calculated by applying finite-differential time domain (FDTD) method. Capacitive electric field due to alternate voltages applied on the RF coils is calculated by successive-over-relaxation (SOR) method. The EM field obtained from the field calculation is substituted repeatedly to Eq. (1). In the present model, 3 turns of antenna coils are small domains corresponding to the cross section of the coil. The antenna voltages are applied on the 1st–3rd coil surface with different amplitude $V_0 = 1800 \text{ V}$, $1800 \text{ V} \times 0.75$, and $1800 \text{ V} \times 0.5$, respectively, in order to take into account the voltage drop due to the inductance and the resistance inside the coil circuit. Time variation of the antenna voltage is given as $V_0 \cos(2\pi\omega_{\text{RF}}t)$.

IV. RESULTS

The spatial distributions of electron (a), proton (b), and H₂⁺ (c) density after a half RF cycle calculation are shown in Fig. 4. The antenna voltage is positive at the first 0.25 RF cycle so that electrons are extracted toward the antenna coil. The electrons, which have initially a uniform spatial distribution, are mainly trapped to the magnetic field line by the rod-filter magnet ($Z = 20 \text{ mm}$, $R = 20\text{--}30 \text{ mm}$) with absolute value 30–120 Gauss (see Fig. 3). This region is around 1st and 2nd turns of antenna coil.

Due to relatively higher electron density in the source chamber ($\sim 10^{16} \text{ m}^{-3}$), the ionization processes of H₂ and H are enhanced. As the dissociation degree of H₂ is given as 0.1, H₂⁺ production rate is an order higher than H⁺ production rate. This leads to the charge balance mainly decided by electrons and H₂⁺ densities.

As the sign of antenna voltage is shifted to negative after 0.25 RF cycle ($t > 1.25 \times 10^{-7} \text{ s}$), the positive charged particles are extracted toward the antenna. This is the reason

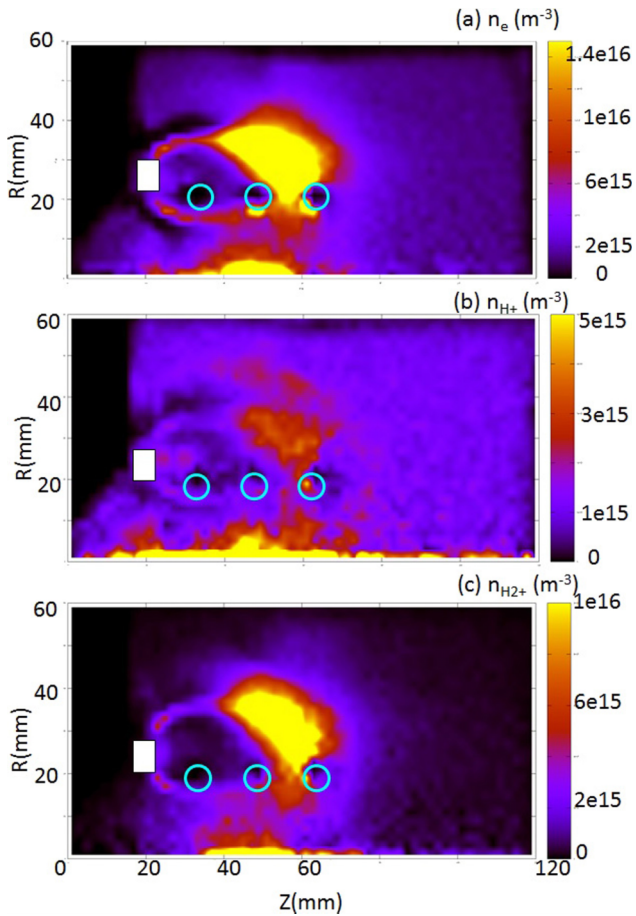


FIG. 4. Spatial variations of electron (a), H^+ (b), and H_2^+ (c) density after 0.5 RF cycle.

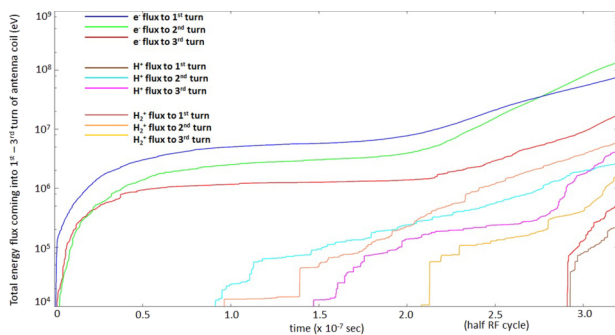


FIG. 5. Total electron, H^+ , and H_2^+ heat flux to 1st–3rd turn of antenna coil.

of the increase in antenna heat flux by H^+ and H_2^+ in Fig. 5. However, still heat flux coming into the antenna is mainly due to electrons in the first half RF phase. Figure 6 shows the average energy of electron, H^+ , and H_2^+ . The high electron heat flux is due to ramp up of the average electron energy. The

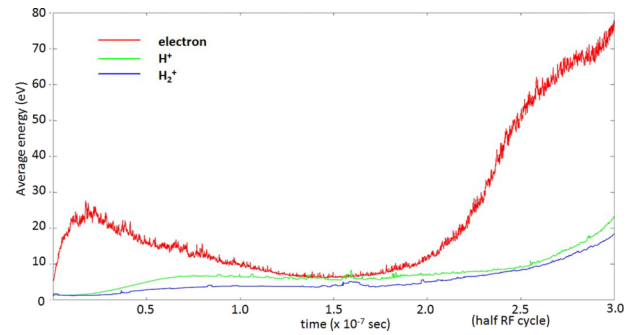


FIG. 6. Time variations of average energy.

time variation of the electron energy is due to fast response of electrons to the capacitive electric field which has maximum and minimum values at $t = 0$ and 2.5×10^{-7} s, respectively.

V. CONCLUSION

A 2D numerical model is developed for plasma transport and EM field in the J-PARC RF IS. A first half RF cycle simulation suggests that the time variation of the plasma heat flux toward the internal antenna coil is due to the following processes: (i) localization of electrons due to the rod filter magnet and due to positive voltage applied on the coil surface, (ii) production of H^+ and H_2^+ by high ionization rate, and (iii) extractions of positive ions due to negative antenna voltage added to electron flux.

It is noticeable that the high plasma density region is produced on the magnetic field line with 30–120 Gauss of absolute magnetic flux density. This results in the higher heat flux onto the 1st and 2nd turns of the coil than 3rd turn. The result suggests that the plasma heat flux onto the antenna can be reduced by changing the magnetic configuration in order to prevent the field line from covering the antenna regions. However, the calculation has been finished for only a half RF cycle. Also, the effect of Cs^+ should be investigated with e^- , H^+ , and H_2^+ . The transport calculation in the steady state with Cs^+ will be reported in the near future.

¹H. Oguri, K. Ohkoshi, K. Ikegami, A. Takagi, H. Asano, A. Ueno, and T. Shibata, “Status of the RF-driven H^- ion source for J-PARC linac,” *Rev. Sci. Instrum.* (these proceedings).

²R. F. Welton, V. G. Dudnikov, B. X. Han, S. N. Murray, T. R. Pennisi, R. T. Roseberry, M. Santana, and M. P. Stockli, *AIP Conf. Proc.* **1515**, 341 (2013).

³A. Ueno, Y. Namekawa, S. Yamazaki, K. Ohkoshi, I. Koizumi, K. Ikegami, A. Takagi, and H. Oguri, *AIP Conf. Proc.* **1515**, 409 (2013).

⁴C. K. Birdsall and A. B. Langdon, in *Plasma Physics via Computer Simulation* (IOP Publishing, Bristol, 1991), Chap. 2, pp. 12–15.

⁵R. K. Janev, D. Reiter, and U. Samm, Juelich Report JUEL-4105, 2003.

⁶K. Nanbu, S. Igarashi, and Y. Watababe, in *Proceedings of Soviet Union–Japan Symposium on Computational Fluid Dynamics* (USSR Academy of Sciences, 1989), p. 126.

⁷T. Takizuka and H. Abe, *J. Comput. Phys.* **25**, 205 (1977).